JOURNAL OF OPTOELECTRONICS AND ADVANCED MATERIALS, Vol. 11, No. 2, February 2009, p. 164 - 168

# Synthesis and characterization of hydrothermally obtained colloidal pseudoboehmite/boehmite

V. JOKANOVIĆ*, B.JOKANOVIĆ[a], B.MARKOVIĆ-TODOROVIĆ, Z.MARKOVIĆ
*Institute of Nuclear Sciences Vinča, Beograd, Serbia*
*[a]Sol Carbon GmBH, Meintigen, Germany*

In this paper, the synthesis and structure of pseudoboehmite/boehmite obtained by hydrothermal method is described. The $SO_4^{2-}$ions were used for the colloid stabilization. The influence of the ageing time on the particle self-assembling from the fibers to the spherical shape of agglomerates has been investigated by using AFM. The started form of the particles immediately after hydrothermal treatment was shown in the form of very elongated fibers with length between 400 and 1000 nm, while the sizes of the spherical particles obtained after ageing during one month were between 140 and 220 nm. The mechanism of obtaining and self-assembling of the fibers into spherical particles has been observed additionally. The TGA and DTA analysis were also done for investigations of the phase transformations during heating treatment of the pseudoboehmite/boehmite samples.

(Received August 15, 2008; accepted February 23, 2009)

*Keywords*: Pseudoboehmite, Boehmite, TGA, DTA, Colloid

## 1. Introduction

During the last years, one-dimensional (1D) nanostructures have attracted many researchers due to their weird properties and applications in nanoscience and nanotechnology [1-3]. In a numerous references, the formation of 1D nanostructure compounds, alumina nanostructure phases (i.e.γ-boehmite, γ and α-$Al_2O_3$) have been reported including various morphologies such as nanotubes [4-5], nanowires [6], nanorods [7-9], nanofibers [10-14], lace-like nanoribbons [15] and plate-like nanostructures[16].

Anisotropic nanostructures with controllable characteristics (phase, size, shape and crystallinity) are of great significance primarily due to their unique properties and potentials quite different from those of the bulk counterparts [1-3]. Recently, much effort has been focused on the preparation of boehmite ( γ-AlOOH) nanomaterials because they can serve as catalyst supports [5], flame retardants [17], adsorbents [18] etc.

Boehmite nanoparticles were used to serve as condensation catalysts to prepare very hard transparent coatings for polycarbonate and an overcoating with polymerizable nanoparticles was used to produce anti-reflective and ultrahard coatings.

Boehmite sols can be prepared by hydrolysis of allkoxides, forced hydrolysis of various aluminium salts or by peptization of aluminium hydroxides. In some references [2-5, 19, 20] have been shown that the properties of boehmite sols, such as particle size, morphology and structure, depend on the type of used aluminium compounds and applied synthesis conditions, preferentially. Some other scientists [22-24] described the preparation of boehmite sols of different shapes and sizes using a hydrothermal peptization of an aluminium hydroxide precipitate. The boehmite sols with spherical particles were obtained by peptizing Al $(OH)_3$ with $HNO_3$ at 252 $^0$C, while hexagonal or fibrillar particles were observed at 282 and 200 $^0$C, respectively.

A hydrothermal method used in our case also was shown as one of the most attractive and promising methods for the synthesis of nanomaterials like boehmite. The powders prepared by this method have good crystallinity and dispersity, and it can be led without significant macroscopic agglomeration of colloid particles [19, 25]. Furthermore, the reaction condition is mild and easy controllable.

## 2. Experimental

### 2.1. Psudoboehmite/boehmite synthesis

Aluminum tri-*sec*-butoxide was dissolved in mixture ethanol /water (ration 1:4). The molar ration aluminum tri-*sec*-butoxide: mixture ethanol-water was 1:50. This mixture was then heated at 85 $^0$C; with vigorous stirring. After 2 h of heating, the solution was cooled to room temperature and the sulfuric acid was added dropwise, while the molar ratio $H_2SO_4$/aluminium tri-sec-butoxide becomes 0.04.. Thereafter, this solution was heated again to 85 $^0$C and refluxed at this temperature for one hour. The obtained colloid solution was immediately after that, transferred into autoclave and conducted under conditions of temperature of the 200 °C and pressure 35 barr during 12 h. After that, the autoclave was cooled down to room temperature.

The solution was then aged for 30 days at normal conditions. Finally, one part of the samples was gelled by very slow drying at 60 °C for 48 h. It was used for

DTA/TGA and XRD investigations, while one part of the sol was diluted more then 100 times for deposition on the surface of the mica substrate for further AFM investigations.

### 2.2. Methods of characterization

The X-ray diffraction (XRD) method (Philips PW 1050) with Cu-$K_{\alpha 12}$ radiation was used for the phase analysis of boehmite/pseudobeoehmite and determination of the crystallite size and lattice parameters. The data were analyzed in the $2\theta$ range from 9 to 90° with a scanning step of $0.05^0$, and exposition time of 2 s per step. The values of the lattice parameters were determined from the characteristic diffraction patterns using the Reitveld full profile method and Koalarie computer software [20,21]. Simultaneously, this program also gives data for the size of the boehmite crystallites based on the Sherer equation

$$d = K\lambda/B\cos\theta,$$

where $d$ (in nm) is the average diameter of the crystallites, $K$ the shape factor, $B$ the width of the (002) diffraction at half maximum height, $\lambda$ the wavelength of the employed X-rays and $\theta$ is the Bragg diffraction angle.

The boehmite/pseudobeoehmite samples were further investigated by differential thermal and thermo-gravimetric analysis, DTA and TGA (AMINCO). The analysis was done in air, with a heating rate of $10^oC$/min.

AFM measurements were performed using Quesant microscope operating in tapping mode in air at room temperature. In tapping mode the cantilever oscillates close to a resonance and the tip only slightly touches the surface. Mica was used as a substrate. boehmite/pseudobeoehmite sol particles were deposited on this substrate and imaged after drying. Standard silicon tips (purchased from Nano and more) with force constant 40 N/m were used. The accuracy of the AFM mean diameter determination was improved by deconvolution. The mean diameter of investigated particles was determined by Quesant SMP program.

## 3. Results and discussion

### 3.1. XRD analysis

The XRD peaks were well matched with γ-AlOOH reported in the JCPDS File No. 21-1307. The average crystallite size of the obtained boehmite powder was calculated through Scherrer formula ($d = 0.9\lambda/B \cos\theta$, where $d$, $\lambda$, $B$ and $\theta$ are average crystallite size, Cu K$\alpha$ wavelength (0.1541 nm), full width at half maximum intensity (FWHM) of (0 2 0) peak in radians and Bragg's diffraction angle, respectively) to be about 4.5 nm using WINFIT program (Fig. 1).

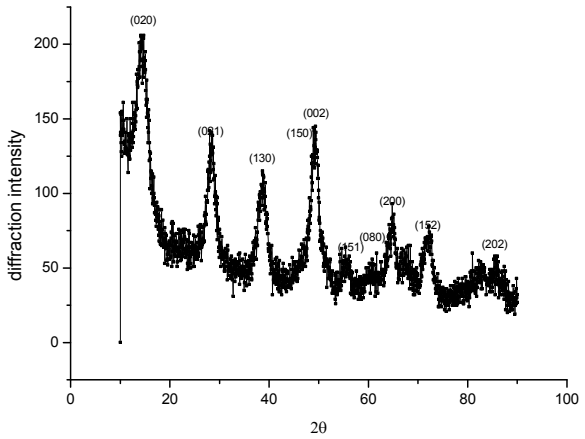


*Fig.1. X-Ray diffraction pattern of boehmite/pseudoboehmite*

All detectable peaks in this pattern can be assigned by their peak position to an orthorhombic γ-AlOOH. Diffraction peak corresponding to the crystallographic plane (020) with maximal corresponding intensity $I/I_0$ lies very closed (only slightly shifted with distance value 0.6135 nm among them) to the values for boehmite (d = 0.61 nm), (Fig. 1). Similar evidence is observed for the other characteristic crystallographic planes (all values of diffraction peaks were slightly shifted more or less (for plane (021) instead of the value of 0.3164 nm it was shifted to the value of 0.3130 nm; for plane of (130) instead of the value of the 0, 2346 nm it was shifted to the value of 0.2332 nm and finally for the plane (002) instead value of the 0,186 nm it was shifted to the value of the 0.1855 nm.).

Obviously that was the evidence that obtained structure of boehmite / pseudoboehmite was much closed to the structures characteristic for clear very well crystallized boehmite. The difference in the structures of our samples and boehmite was negligible. Following the literature, that kind of structure was characteristic for well crystallized samples and for a slightly more elongated fibrous boehmite which structure is only slightly defected, on the opposite to the pseudoboehmite structure, which is characterized by more defected structures of very small particles with dominant shape of the rods or needles, with a sizes of range less than 10 nm. When the shift of diffraction peak to the value corresponding to pseudoboehmite is more pronounced, the crystallinity is lower because the pseudoboehmite has lower crystallinity compared to boehmite. Buining et al. [26, 27] have found that this diffraction peak shift is a consequence of the change in interlayer water content. In accordance to this, the shift to the higher d values and pseudoboehmite phase can be expected for higher the interlayer water content.

This suggests that the amount of $H_2SO_4$ added for peptization plays an important role not only in the stabilization of sol, but also in changes in the crystal structure of powders and if its quantity is lower, it can be expected that the structure might be shifted more to the typical boehmite structure. From some information given

in literature the average size of was also important for the structure shifting from the boehmite structure. For so small boehmite/pseudobohmite crystallite of the average size (4, 5 nm) the serious shifting can be expected.

In spite of this, probably thanking to the strong hydrothermal treatment the shifting of the structure is negligible. That fact of so small crystallite sizes led to clear evidence that the boehmite/pseudoboehmite fibers were consisted from a large number of the crystallites which have the preferential way of the crystallization along one way, following the direction of the $OH^-$ ions on the ends of the pseudoboehmite/boehmite zig zag chains.

The crystal structure of boehmite consists of an orthorhombic unit cell (a = 2.86, b = 12.24, c = 3.69 A °) in which all the atoms, with the exception of H, locate at the 4c positions thereby having four formula units per cell. Each Al is coordinated by 6 O to form an octahedron, and the edge-sharing octahedra are arranged to form an interlocking double layer, as shown in Fig 2.. The layers are linked together by hydrogen bonds in an array of linear zigzag chains parallel to the c-axis [26]

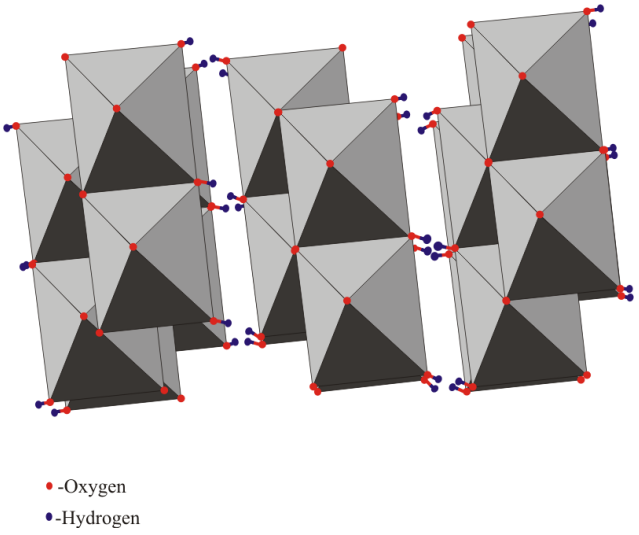


*Fig.2. Unit cell of boehmite. The zigzag H-O…H-O spots shows schematically zigzag chains of H-bonds.*

### 3.2. TGA/DTA analysis

The DTA–TG curve of the dried gel powder is shown in Fig.3... In the temperature range 50–300 $^0$C DTA curve shows a broad endothermic peak at 180.7 $^0$C, a sharp exothermic peak at about 293.1$^0$C and another endothermic peak at 290 $^0$C. At higher temperature, the DTA curve shows a sharp and sharp endothermic peak at about 477 $^0$C. (Fig.3 and Fig.4)

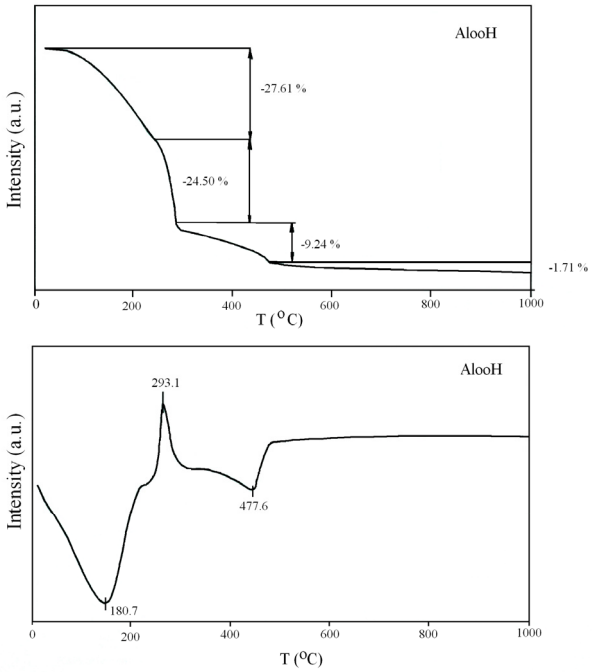


*Fig.3. DTA and TGA curve of pseudoboehmite/boehmite*

The TG curve of the gel shows a gradual weight loss of about 27.61 mass % in the temperature range 25–180.73 $^0$C and another weight loss of about 24.50 mass % in the temperature range 180.7–293.1$^0$C show a further weight loss of 9.24% mass % which takes place in third stage.

Thus, the first endothermic peak and the associated weight loss correspond to the loss of physically adsorbed water inside of very fine pesudoboehnime/boehmite nanopores. The second exothermic can be associated to the crystallization of bayerite ($\beta$-$Al_2O_3$ $3H_2O$).[28] The third endothermic peak undergoes further dehydroxylation bayerite to pseudoboehmite/boehmite $\gamma$-AlOOH in the temperature range 293.1–477.6 $^0$C dehydroxylation of pseudoboehmite. The theoretically expected weight loss was 19.61mass %. The difference was caused by the subsequent forming the aluminium-hydrate chains, which includes the generation of the trimmers and tetramers structures and obviously corresponding less weight loss.

### 3.3. AFM investigations

In the first phase, immediately after hydrothermal treatment the particles of pseudoboehmite have form of entangled long fibers, as it can be seen in Fig.5.The length of these fibers were 400-1000 nm and depth about 20 nm. They were tailed with clear intergrowth with formation of the new branches on one the bigger entangled fiber of pseudoboehmite.

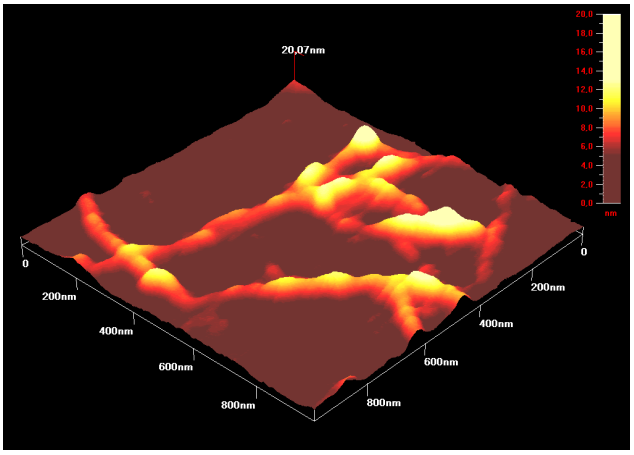


*Fig.4. Typical appearance of pseudobeohmite/boehmite fibers*

After one month ageing the three-dimensional network of the fibers was formed as it can be seen in the Fig.6. The prevailing shape was spherical or mildly polygonal shape. The particles have sizes in the range 140-220 nm.

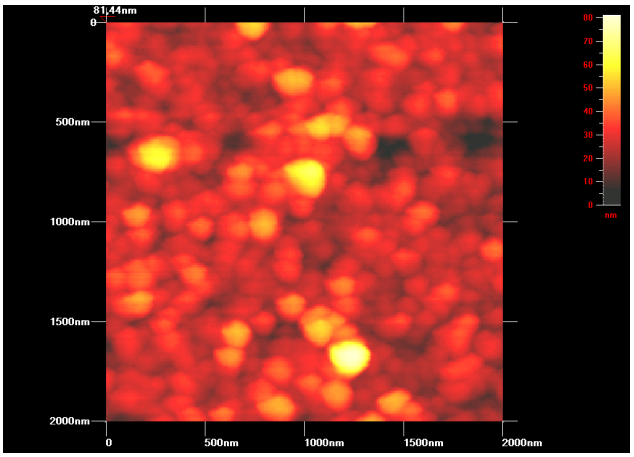


*Fig.5.Typical appearance of pseudoboehmite particles after ageing during one month.*

Only some small part of them has the sizes a slightly bigger approximately around of 350 nm (see Fig.6).

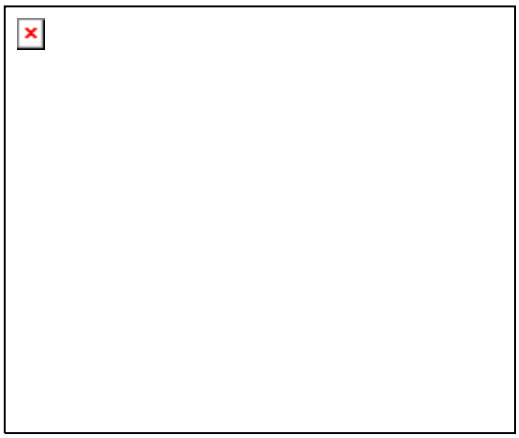

*Fig.6. Distribution of pseudoboehmite/boehmite particles after ageing during one month*

### 3.4. The mechanism of generation of pseudoboehmite network and capsule shape

The orthorhombic structures γ -AlOOH has a distinctive layered structure of γ-AlOOH lamellar [13]. In this structure, one monolayer is one layer of deformed octahedra with an aluminum atom near their center, two hydroxyls and four oxygen atoms in their vertices. The coordination geometry around the oxygen ions corresponds to a distorted tetrahedron. The octahedral joined by edges result in AlO(OH) polymeric layers. These layers are held together by hydrogen bonds between the $OH^-$ groups of each octahedron. The $OH^-$ groups within the structure could form zigzag chains between the planes of oxygen ions. With the distinctly layered structures, boehmite possesses a preferential growth direction with the lowest growth energy. This makes the crystal growth along the certain direction.

In addition, this weak interaction between two double layers causes the crystal surface to end in the interface, producing surfaces full of hydroxyls [8, 29]. The driving force of the formation of nanofibers by assembling nanoparticles possibly originates from the hydrogen bonds on the surface of nanoparticles via oriented attachment mechanism. So the above surfactant/ligand-free exclusive anisotropic growth habit of nanofibers can be understood from the view-point of the intrinsic structure of the boehmite.

With increasing the temperature, in the nonequilibrium solution of autoclave at the initial stage of the hydrothermal reaction small nanoparticles have been gradually dissolved to generate free ions in the solution, and spontaneously transferred onto the surfaces of some large nanoparticles. Due to the free energy difference for the particles with the different size, the larger nanoparticles grew at the cost of the smaller particles through Ostwald ripening, according to the well-known Gibbs–Thomson law [8, 20, 25, 30]. Continuing this ripening process the starting nanoparticles gradually arranged along the main crystallographic axes to form nanofibers via an oriented attachment mechanism (Fig 4.), finally forming the longer nanofibers.

From the other side, these fibers were very strongly entangled, causing the self assembling of the fibers in the various ways giving at the end the three dimensional spherical shape to the network of obtained agglomerates, caused partially by relatively high concentration of pseudoboehmite/boehmite particles.

If the concentration of sulfate ions is not enough high the interaction of the Al-O polynuclear species in the capsule shell is week and the strong interactions between the number nanocapsules is not so strong to prevent their aggregation. The stronger interaction between the nanocapsules provides the growth of the capsules with bungled pseudoboehmite/boehmite fibers and some extent of their aggregation in the form of spherical/polygonal shapes (Fig.5).

In the first phase the mono-layer sols show a flat network of single interwoven fibrils of pseudoboehmite. During the next phase two-layer sol was formed with

interwoven the single fibrils, and a large number of long, thick bundles of parallel fibrils that can not be disperse with stirring. The last phase was formation of the three-dimensional network in the interior of the aqueous sols, which was possible through of one month ageing of the relatively concentrated pseudoboehmite sol. [19, 20, 25, 30].

This process was additionally supported by small capillary forces inside of the capsule of pseudoboehmite and fluid instability and its disturbance, which provide insertion of very small pseudoboehmite particles into open channels of bigger particles inside of their three-dimensional network in shape of capsules, as it is presented in Fig.5 and Fig.6. When the capsules were enough grown, the process was ended, because they were enough big and the previous mechanism of infiltration of small particles into a network of bungled pseudoboehmite fibers was not possible to be continued

## 4. Conclusions

Hydrothermal process of obtaining of pseudoboehmite/boehmite sol was investigated in this paper. The fibers shape of obtained particles immediately after hydrothermal treatment was dominant and spherical shape was dominant after ageing during one month.

The mechanism of self assembling during transformation from the fiber to the spherical form was investigated by using AFM.

The structure and phase composition of the pseudoboehmite/boehmite particles were investigated by using XRD and TGA/DTA investigations.

**Acknowledgment**

This work was supported by Ministry of Scinece and Technology of the Republic Serbia through project No. 142070.

## References

[1] Helmut Schmidth, Appl. Organometal. Chem. **15**, 331 (2001).
[2] Xiang Ying Chena, Solid State Communications **145**, 368 (2008).
[3] I. S. Park, M. S. Kwon, N. Kim, J. S. Lee, K. Y. Kang, J. Park,Chem. Commun. 45, 5667 (2005).
[4] Y. F. Mei, X. L. Wu, X. F. Shao, G. S. Huang, G. G. Siu, Physics Letters A, **309**, 109 (2003).
[5] H. C. Lee, H. J. Kim, S. H. Chung, K. H. Lee, H. C. Lee, J. S. Lee, J. Am.Chem. Soc. **125**, 2882 (2003).
[6] Xiang Ying Chen, Hyun Sue Huh, SoonW Lee, Nanotechnology **18,** 285608 (2007).
[7] Yi-Pei Lee, Yi-Hsin Liu and Chen-Sheng Yeh, Phys. Chem. Chem. Phys. **1**, 4681 (1999)
[8] Ali Mohraz *, Michael J. Solomon, Journal of Colloid and Interface Science **300**, 155 (2006).
[9] R. Petrovic, S. Milonjic, V. Jokanovic, Lj. Kostic-Gvozdenovic, I. Petrovic-Prelevic, Dj. Janackovic, Powder Technology **133**, 185 (2003).
[10] Jian-Feng Chen, Lei Shao, Fen Guo, Xing-Ming Wang, Chemical Engineering Science **58**, 569 (2003).
[11] F.P. Faria, P. Souza Santos, H. Souza Santos, Materials Chemistry and Physics **76**, 267 (2002)
[12] Yuanyuan Li , Jinping Liu, Zhijie Jia, Materials Letters **60**, 3586 (2006).
[13] Jun Zhang, Fengjun Shi, Jing Lin, Si Yi Wei, Dongfeng Chen, Jian Min Gao, Zhixin Huang, Xiao Xia Ding, Chengcun Tang, Materials Research Bulletin **43**, 1709 (2008).
[14] H. Y. Zhu, J. D. Riches, J. C. Barry, Chem. Mater. **14**, 2086 (2002).
[15] S.C. Shen, W.K. Ng, Q. Chen, X.T. Zeng, Reginald B.H. Tan, Materials Letters **61**, 4280 (2007).
[16] Hamed Arami, Mahyar Mazloumi, Razieh Khalifehzadeh, S.K. Sadrnezhaad, Journal of Alloys and Compounds **461**, 551 (2008).
[17] G. Camino, A. Maffezzoli, M. Braglia, M. De Lazzaro, M. Zammarano, Poly. Degrad. Stab. **74**, 457 (2001).
[18] S. Tanada, M. Kabayama, N. Kawasaki, T. Sakiyama, T. Nakamura, M. Araki, T. Tamura, J. Coll.Interface Sci. **257,** 135 (2003) .
[19] Xim Bokhimi, Antonio Morales, Jaime S. Valente, J. Phys. Chem. C **111**, 103 (2007).
[20] Pramod K. Sharma,V.V. Varadan,V.K. Varadan, Journal of the European Ceramic Society **23**, 659 (2003).
[21] D. Panias, A. Krestou, Powder Technology **175**, 163 (2007).
[22] S.K. Milonjic, Sci.Forum, **214**, 197 (1996).
[23] M. Dj. Petkovic, S.K. Milonjic, V.T. Dondur, Bull. Chem. Soc. Jpn. **68**, 2133 (1995).
[24] Maria Lúcia Pereira Antunes, Helena de Souza Santos, Persio de Souza Santos, Materials Chemistry and Physics **76** 243 (2002).
[25] C. P. Nicholas, H. Ahn, T. J, Marks, J. Am. Chem. Soc. **125**, 4325 ( 2003).
[26] C.-K. Loong, M. Ozawa, Journal of Electroanalytical Chemistry **584**, 5 (2005).
[27] X. Bokhimi, J. A. Toledo-Antonio, M. L. Guzmán-Castillo, B. Mar-Mar, F. Hernández-Beltrán, J. Navarrete, Journal of Solid State Chemistry **161**, 319 (2001).
[28] Qian Liu, Aiqin Wang, Xiaodong Wang, Tao Zhang, Microporous and Mesoporous Materials **92**, 10 (2006).
[29] S. Music, O. Dragcevic, S. Popovic, Materials Letters **40**, 269 (1999).
[30] Geik Ling Teoh, Kong Yong Liew, Wan A.K.Mahmood, Journal of Sol-Gel Science and Technology, **44**(3), 177 (2007).

*Corresponding author: vukoman@vin.bg.ac.yu